Aggregation Behavior of a Symmetric, Fluorinated, Telechelic Polymer System Studied by ^{19}F NMR Relaxation

J. Preuschen,[†] S. Menchen,[‡] M. A. Winnik,[§] A. Heuer,[†] and H. W. Spiess*,[†]

Max-Planck-Institut für Polymerforschung, Ackermannweg 10, 55128 Mainz, Germany, Applied Biosystems Division, Perkin-Elmer Corporation, 850 Lincoln Centre Drive, Foster City, California 94404, and Department of Chemistry, University of Toronto, Toronto, Canada, M5S 3H6

Received December 2, 1998; Revised Manuscript Received February 5, 1999

ABSTRACT: ^{19}F NMR experiments are used to study the aggregation behavior of two telechelic polymer systems. These polymer systems consist of a water−soluble chain, here poly(ethylene glycol), with two hydrophobic endgroups. Because of the hydrophobic interaction of the fluorocarbon endgroups, these polymer chains associate in water to form aggregates at low concentrations. The aggregate comprises a core formed from the insoluble hydrophobic endgroups that are surrounded by a corona of long water-soluble polymer chains. With increasing polymer concentration, the polymer chains start bridging so that a three-dimensional, physical network with fluorinated aggregate cores as cross-link points is formed. This effect can be substantially enhanced by replacing the hydrophobic endgroup C_6F_{13} with C_8F_{17}, a consequence of the stronger association of C_8F_{17} in aqueous solution. By different ^{19}F NMR parameters, i.e., ^{19}F transverse relaxation and ^{19}F chemical shift, we can distinguish aggregated and nonaggregated chain ends. This enables us to follow the formation of an infinite network.

Introduction

In a recent paper,[1] the synthesis, characterization, and rheological behavior of a concentration series of poly(ethylene glycol)s (PEG) end-capped with fluorocarbon hydrophobes samples was reported. Beyond the fluorinated endgroups, a flexible polymer chain exists and consists of hydrophilic PEG which is attached via isophorone diisocyanate, IPDI.[1] The hydrophilic character is based on the PEG−water interactions.

The unusual aggregation behavior of telechelic polymer systems in general is studied with light scattering, fluorescence spectroscopy, and rheology experiments,[1−10] but none of these methods is specifically sensitive toward the hydrophobic endgroups. By using nuclear magnetic resonance spectroscopy (NMR), the endgroups, containing fluorine (^{19}F), the main chain, containing protons (^{1}H), and the solvent, containing deuterated water (^{2}H), can be monitored separately. Thus, we are able to observe directly the aggregation behavior of the fluorinated endgroups with ^{19}F NMR. Because of the low sensitivity of NMR, we can only probe samples with polymer concentrations (1−10 wt %) far above the critical aggregation concentration (CAC). From Xu et al.,[1] we know that at about 0.06 wt % two species with two different diffusion constant are present for PEG−$(C_6F_{13})_2$.[1] At this concentration, which could be identified as the CAC, the aggregation process starts. According to common surfactant theories, the CAC is determined by the fraction of free molecules which stays constant over the whole concentration series.[11,12] The length of the C_6F_{13} and the C_8F_{17} endgroup is around 0.65 and 0.91 nm.[13] At 303 K, the hydrodynamic radius R_H of an unmodified PEG chain with $M_w = 35\,000$ g/mol is calculated to be 5.7 nm.[14]

In this paper, we focus on the aggregation process in an advanced state and ultimately on the formation of the infinite network. By different ^{19}F NMR parameters, i.e., ^{19}F transverse relaxation and ^{19}F chemical shift, we can distinguish aggregated and nonaggregated chain ends. This enables us to follow the formation of an infinite network by the aggregation of the fluorinated endgroups and compare this with simulation results. The aggregation behavior of different endgroups C_6F_{13} and C_8F_{17}, respectively, can also be compared by such experiments. Additionally, with ^{19}F NMR experiments, we can study easily the temperature dependence of the aggregation process and compare it with the aggregation behavior of nonionic surfactants.

The paper is organized as follows. In NMR Theory, information on NMR relaxation in solids and liquids is outlined. Sample preparation and the NMR setup is briefly described in the Experimental Section. The data from the ^{19}F NMR experiments are presented in Results. The Discussion section combines the experimental results with a theoretical treatment of an infinite network and leads to the description of a microscopic picture of the aggregation behavior of such telechelic polymers.

NMR Theory

We begin with a short introduction to NMR and NMR relaxation. The ^{19}F nucleus investigated has a nuclear spin $I = {}^1/_2$. Therefore we are dealing with dipolar interactions among spins with $I = {}^1/_2$. After a 90° pulse or after more complicated pulse sequences, relaxation of the magnetization takes place. The loss of nuclear magnetization occurs by different pathways for solids and liquids, but in both cases, the NMR relaxation occurs mainly via fluctuations of the dipolar coupling among the spins.[15−18]

In the case of liquids, rapid motion leads to spin lattice relaxation with the relaxation time T_1 and a transverse relaxation with the relaxation time T_2. Both are described by the Bloembergen−Purcell−Pound (BPP) theory.[19] In liquids, the dipolar interaction among nuclei with $I = {}^1/_2$ is averaged to zero because of the isotropic

* To whom correspondence should be addressed.
† Max-Planck-Institut für Polymerforschung.
‡ Perkin-Elmer Corporation.
§ University of Toronto.

10.1021/ma9818735 CCC: $18.00 © 1999 American Chemical Society
Published on Web 03/31/1999

motion of molecules. For the type of fast motion common to liquids, the spin lattice relaxation rate $1/T_1$ and the spin−spin relaxation rate $1/T_2$ are equal:

$$\frac{1}{T_1} = \frac{1}{T_2} = \frac{3}{2}\left(\frac{\mu_0}{4\pi}\right)^2 \frac{\gamma^4 \hbar^2}{r^6} \tau_c \qquad (1)$$

where μ_0 is the magnetic field constant in a vacuum, γ is the gyromagnetic ratio of the investigated nuclei, r is their internuclear distance, and τ_c is the correlation time that is determined primarily by the motion in liquids.

For liquids, the BPP theory predicts an exponential relaxation for the transverse relaxation, called free induction decay (FID):

$$G(t) = \exp\left(-\frac{t}{T_2}\right) \qquad (2)$$

where $G(t)$ is the relaxation function. The Fourier transform of this expression leads to a Lorentzian line shape for the spectra of liquids. In gels, the line shape is actually more complicated because of the presence of residual dipolar couplings.[20] This does not enter into our analysis, however, because only transverse relaxation of *magnetization* is studied.

We chose for this investigation of self-assembling model networks ^{19}F NMR relaxation based on pulse sequences with one or two pulses. A 90° pulse generates a FID, whereas the two pulse sequence, a 90° pulse is followed by a 180° pulse, generates an echo of the transverse magnetization M_x. This 90°−180° pulse sequence refocuses the interactions linear in I_z (inhomogenity of the B_0-field, chemical shift, and heteronuclear dipolar coupling) and emphasizes the nuclei which are not dipolar coupled.

Experimental Section

^{19}F NMR Experiments. The ^{19}F NMR experiments were performed on a Bruker DSX 300 spectrometer with a home-built single resonance static probehead at a ^{19}F resonance frequency of 282.5 MHz. The $\pi/2$ pulse duration was 4 μs for an inner coil of 5 mm. The material used for the probehead was Vespel instead of PTFE [poly(tetrafluoroethylene)]. Vespel does not contain fluorinated polymers. $CFCl_3$ was used as an external standard (0 ppm).

The ^{19}F transverse relaxation was recorded in a 2D experiment, using the 90°−τ−180°−τ pulse sequence and measuring the amplitude in the other dimension. This relaxation function is called the transverse relaxation. The pulse spacing τ was varied between 10 μs and 50 ms for fluorine.

Sample Preparation. The synthesis and characterization of the fluorocarbon endcapped poly(ethylene glycol) PEG−$(C_6F_{13})_2$ and PEG−$(C_8F_{17})_2$ is described elsewhere.[1] The fluorocarbon endgroups are attached to the PEG chains via isophorone diisocyanate:

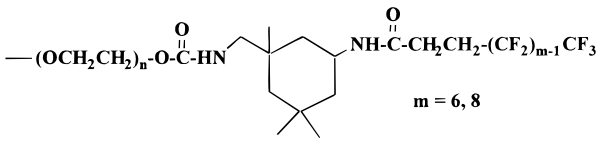

The PEG polymer has a molecular weight of 35 kg/mol (≈800 monomers). The experiments were carried out in a series of six PEG−$(C_6F_{13})_2$ solutions with polymer concentrations of c_{pol} = 1.7, 2.5, 4.1, 5.8, 6.4, 8.8, 9.6, and 20 wt % in the solutions. Deuterated water (99.9%) purchased from Merck GmbH (Darmstadt, Germany) was used as a solvent. The second sample series contains three PEG−$(C_8F_{17})_2$ solutions with c_{pol} = 1.5, 4.8, and 9.8 wt % polymer. The polymer was weighed directly into an NMR tube. Then, the solvent was added, and its weight was determined. The NMR tube was sealed under vacuum to be sure that no D_2O evaporated and that the PEG did not react with oxygen. After centrifuging, the solutions were allowed to stand at room temperature in the dark for at least three months until the ^1H NMR relaxation, checked at weekly intervals, reached a constant behavior and the solution was clear. Thus we are dealing here with *aged* samples.

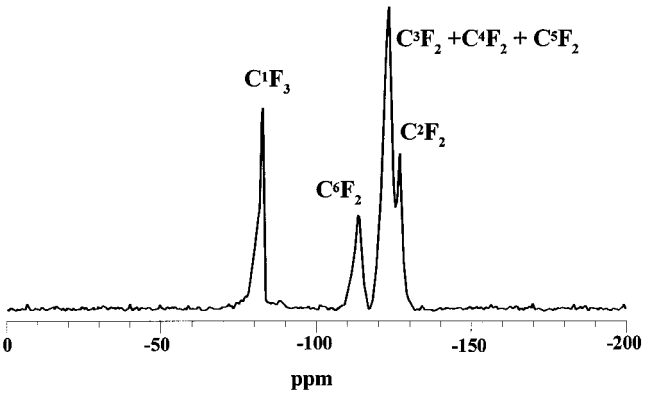

Figure 1. ^{19}F spectrum of PEG−$(C_6F_{13})_2$ with c_{pol} = 6.4 wt %. The peaks are assigned to the chemical groups along the chain as indicated.

Results

To examine the association behavior of the PEG samples with the two different endgroups C_6F_{13} and C_8F_{17}, we present the ^{19}F NMR relaxation data for both sample series. The ^{19}F NMR measurements provide information on the aggregate cores formed through association by these telechelic polymer systems. To study the dynamic of this fluorocarbon core, we employed the transverse relaxation.

$$C^1F_3-C^2F_2-C^3F_2-C^4F_2-C^5F_2-C^6F_2-CH_2-CH_2-O-$$
1

Figure 1 shows a spectrum of PEG−$(C_6F_{13})_2$ with c_{pol} = 6.4 wt %. The notation used to denote the various positions along the chain is shown in **1**. The peaks are assigned relative to $CFCl_3$ (0 ppm) as an external standard as follows: −81 ppm (C^1F_3), −113 ppm (C^6F_2), −123 ppm (C^3F_2, C^4F_2 and C^5F_2), −126 ppm (C^2F_2), taken from the work of Cochin et al.[21] The signals of the three CF_2 groups (third, fourth, and fifth) overlap to form a single resonance. For a polymer concentration below 6.4 wt %, it is also possible to assign a unique chemical shift to C^4F_2 (−122 ppm). The assignment follows the fluorocarbon chain from the center (first group) of the core to the corona core interface (sixth group). The first chemical group is the C^1F_3 group, and the chain ends with the C^6F_2 group. This last group is the one that forms the link to the PEG chains. Compared to other CF_2 groups, a difference is seen in the line broadening of the assigned peak.

^{19}F NMR Transverse Relaxation. Each transverse relaxation of PEG−$(C_6F_{13})_2$ exhibits a nonexponential decay profile: a fast decay followed by a longtime exponential tail. The curves were fitted with the biexponential function:

$$A_{short} \exp(-t/T_{2,short}) + A_{long} \exp(-t/T_{2,long}) \qquad (3)$$

where $A_{short} + A_{long} = 1$, $T_{2,long}$ describes the decay time of the long decay, and $T_{2,short}$ may be thought of as an

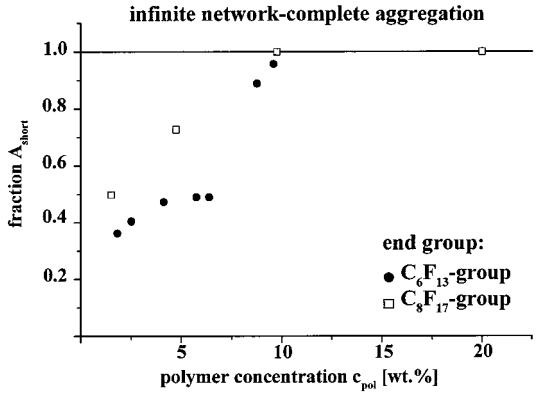

Figure 2. Fraction A_{short} fitted from the transverse relaxation of PEG−$(C_6F_{13})_2$ and PEG−$(C_8F_{17})_2$ plotted against the polymer concentration. For both polymer systems, this fraction increases up to 100% with increasing polymer concentration.

average relaxation time describing the faster relaxation processes. The values for the long relaxation time $T_{2,long}$ are about 2 ms with little variation in the series and significant correlation to c_{pol}. For the short relaxation time $T_{2,short}$, we find values around 200 μs, which is a factor 10 shorter than $T_{2,long}$. In Figure 2 the fraction A_{short} is plotted against the polymer concentration c_{pol} in wt %. This fraction increases up to 100% with increasing polymer concentration.

We also recorded the transverse relaxation of the polymer system in bulk at room temperature employing the same pulse sequence. The ^{19}F relaxation follows an exponential function with T_2 equal to 210 μs (fraction = 1). Thus the relaxation times of the bulk and the dissolved samples are similar for $T_{2,short}$. It is worth noting that for the bulk sample at room temperature the PEG domain is largely crystalline (studied by DSC), but the relaxation time observed does *not* correspond to highly crystalline fluorinated domains but to amorphous domains.

For the sample with two additional CF_2 groups in the endgroup, we find a similar relaxation behavior. The relaxation curves of PEG−$(C_8F_{17})_2$ with c_{pol} = 1.5 and 4.8 wt % are biexponential, whereas the relaxation of 9.8 wt % is monoexponential with a relaxation time T_2 of 271 μs. The longer relaxation time $T_{2,long}$ is equal to ca. 2 ms. The fraction A_{short} of PEG−$(C_8F_{17})_2$ is also plotted in Figure 2. Again this fraction increases with increasing polymer concentration. Because we find for PEG−$(C_8F_{17})_2$ the same relaxation times as those for PEG−$(C_6F_{13})_2$, there is almost no change in the mobility of the fluorocarbon endgroup at any concentrations of PEG-$(C_8F_{17})_2$ compared to those of PEG-$(C_6F_{13})_2$.

Temperature Dependent ^{19}F NMR Spectra. To probe the temperature-dependent aggregation behavior of the fluorocarbon endgroups, ^{19}F NMR spectra for PEG-$(C_6F_{13})_2$ were recorded over a temperature range of 70 K above room temperature. At T = 303 K only four of the six chemical groups are resolved in Figure 3. The resonances are broadened because of the slow motion of the fluorocarbon groups. Increasing the temperature to T = 363 K results in considerably improved spectral resolution. The six well-resolved peaks are assigned to the chemical groups according to Cochin et al.[21]

The second effect of the temperature increase concerns the chemical shift of each group. From literature, it is well-known that the chemical shift of fluorine is a very sensitive indicator of aggregation phenomena.[22−25]

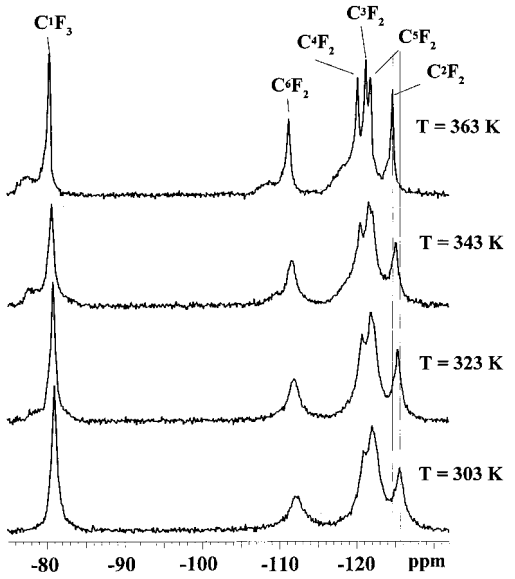

Figure 3. Temperature dependent ^{19}F NMR spectra of PEG−$(C_6F_{13})_2$ in D_2O with c_{pol} = 9.6 wt %. At room temperature, the absorption lines are broadened, and only four peaks are resolved. The resolution is improved by increasing the temperature. At a temperature of 363 K, the six chemical groups of the fluorocarbon endgroups are resolved and can be assigned.

For surfactants containing fluorocarbon groups, Guo et al.[25] found that below CAC each chemical group is resolved. Increasing the surfactant concentration leads to a signal increase proportional to the concentration of free surfactants. Upon reaching the critical aggregation concentration, a second peak for each group appears. This set of peaks is attributed to the aggregated chain ends. In the aggregates, the nuclei are more shielded, and therefore, the chemical shift decreases. Additionally the peaks are broadened compared to the first set of peaks. The chemical shift difference of the aggregated and nonaggregated species was found to be 2.41 ppm for the C^1F_3 group and 0.9−1.82 ppm for the CF_2 groups, where the nonaggregated species have higher shifts.

In the telechelic polymer system studied here, the two sets of peaks are not resolved. However, a marked temperature dependence of the chemical shift of all lines is observed. The aggregation behavior is studied in detail by the chemical shift of the C^3F_2 group which exhibits a total difference of $\Delta\delta$ = 1.6 ppm, equivalent to that found by Guo et al.[25] Thus we attribute the chemical shift at high temperatures to the nonaggregated species and the temperature dependence of the chemical shift to an increasing concentration of free chains with increasing temperature. Because single lines are observed, the chemical shift δ_{obs} results from a weighted superposition of the signals of aggregated and free endgroups:

$$\delta_{obs} = c_{free}\delta_{free} + c_{agg}\delta_{agg} \quad (4)$$

with $c_{free} + c_{agg} = 1$. The values of δ_{agg} and δ_{free} are taken from the sample with the highest concentration at 295 K and the lowest concentration at 370 K, respectively. With this assignment, the fraction of the nonaggregated chain ends is determined as a function of temperature for several concentrations.

The results for the polymer system PEG−$(C_6F_{13})_2$ with c_{pol} = 1.7, 5.8, and 9.6 wt % are collected in Figure

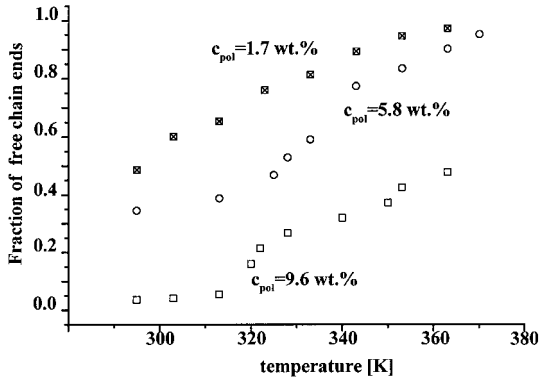

Figure 4. Fractions of free chain ends of PEG−$(C_6F_{13})_2$ as a function of temperature determined from ^{19}F NMR chemical shift for three different polymer concentrations: $c_{pol} = 1.7$, 5.8, and 9.6 wt %. Note the cascade increase of free chain ends at $T = 320$ K for $c_{pol} = 9.8$ wt % and $T = 340$ K for $c_{pol} = 5.8$ wt %, respectively.

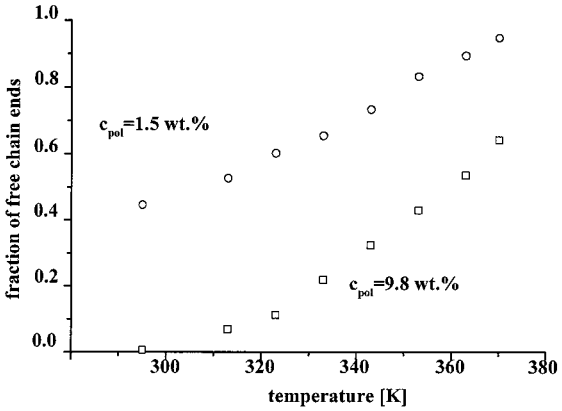

Figure 5. Fractions of free chain ends of PEG−$(C_8F_{17})_2$ as a function of temperature determined from ^{19}F NMR chemical shift for two different polymer concentrations $c_{pol} = 1.5$ and 9.8 wt %.

4. The plot clearly shows the significant increase of the fraction of free chain ends with increasing temperature. For the low- and intermediate-concentration sample with $c_{pol} = 1.7$ and 5.8 wt %, we find almost no aggregated endgroups at high temperatures, whereas in the high concentration sample, half of the endgroups are still aggregated.

The results for the polymer system PEG−$(C_8F_{17})_2$ with $c_{pol} = 1.5$ and 9.8 wt % are collected in Figure 5. The temperature dependence is similar to that of PEG−$(C_6F_{13})_2$. Note that in both cases our experiments at room temperature are performed at concentrations above CAC. Thus, the fraction of free chain ends is expected to be below 0.5, as is indeed observed.

Discussion

Assignment of T_2 to the Aggregated and Nonaggregated Endgroups. We first discuss the results of the ^{19}F NMR transverse relaxation. For all solutions of PEG−$(C_6F_{13})_2$, we find that the short relaxation time $T_{2,short}$, occurring with weight A_{short}, is for both polymer systems equal to the bulk sample. Therefore, A_{short} is a direct measure for the fraction of aggregated species. Because the relaxation times in solution and in bulk are similar to each other, the structure and the resulting dynamics of the fluorinated cores must be close to those found in the solid polymer. $T_{2,short}$ has a value of ~200 μs for both PEG systems, and it seems to be the typical relaxation time for aggregates of *both* systems. The second relaxation time $T_{2,long}$ of the polymer solutions is around 2 ms.

From literature, it is known that "dissolved" hydrophobic molecules form a clathrate cave with water molecules.[11,12] This cave slows down the dynamic processes of the dissolved fluorinated endgroup and explains the rather short $T_{2,long}$ of 2 ms. Second, we cannot distinguish between free chain ends and weakly aggregated (e.g., two endgroups) chain ends which built up "loose" or random aggregates.[26]

After identifying the immobile endgroups as aggregated endgroups forming *stable*, solidlike cores, we now can analyze the experimental data shown in Figure 2. The fraction of aggregated species is increasing with increasing polymer concentration. In the case of polymer surfactants, there is a dramatic decrease of the free and weakly aggregated chain ends for both polymer systems.

Shape of the Aggregates. Several possible aggregation states exist for polymer surfactants at high polymer concentrations. The first one is defined by the flower micelles which are built up by loops (ring conformation of the polymer chain). The formation of flower micelles is well-described by the common surfactant theory,[11,12] because all polymer molecules aggregate as soon as CAC is reached except the small amount of polymer molecules which are equal to the CAC. Therefore, we would expect that, e.g., at $c_{pol} = 5$ wt % $\gg$ CAC, less than 1% of the endgroups are free. If on the contrary we assume micelles in which only one end of the polymer chains is aggregated and the other chain end is free, we would expect that for each concentration 50% of the chain ends are aggregated, for all concentration $c \gg$ CAC. Clearly, both expectations are at variance with the concentration- and temperature-dependent fractions of aggregated species for both polymer systems. Therefore, another aggregation model is needed to explain the results. Indeed, Raspaud et al. mentioned the formation of "loose" or random aggregates where the fraction of free chain ends is not well defined because of the undefined structures that are possible.[26] With the formation of "loose" aggregates, the low aggregation number can easily be explained.

In Figure 6, a schematic aggregation diagram of symmetric telechelic polymer systems summarizes the different aggregation processes. For small polymer concentrations, only single polymer chains, known as unimers, are found. Increasing the polymer concentrations leads to two different aggregation phenomena: (a) formation of micelles and (b) formation of random aggregates. Evidently, the polymer systems studied here follow the latter path. Both aggregation processes end with the formation of an infinite network which is considered in the next section.

Network Formation through Aggregation. Next we discuss the formation of a three-dimensional network by complete aggregation of the chain ends. In Monte Carlo simulations of symmetric A−B−A triblock copolymers in a good solvent for B and a bad solvent for A, Nguyen-Misra et al.[27,28] found that the critical gel concentration in terms of volume fractions Φ_{Gel} is equal to $\Phi_{Gel} = 0.1\alpha^{-0.14}$. Here, α characterizes the hydrophobic interaction of the endgroups. The incompatibility is determined by the length of the two endgroups and by the interaction energy of water with fluorine. Experimentally, α is determined for one CF_2 group to be $1.5kT$.[29,30] Thereby, we neglect the hydrophobic influ-

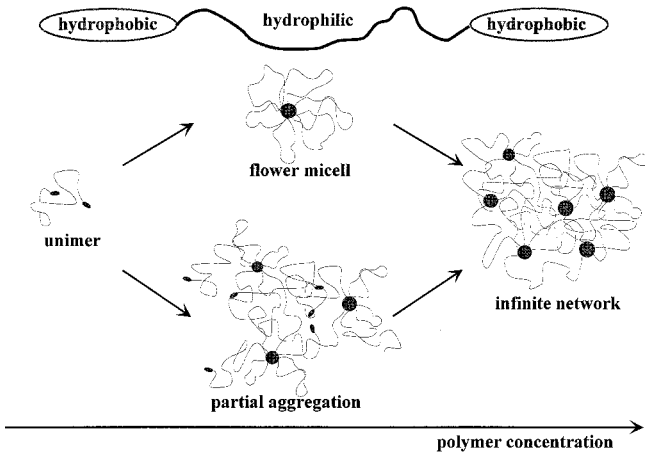

Figure 6. Aggregation pathways. For telechelic polymer systems, two different aggregation processes exist above CAC. The upper path represents the formation of flower micelles, whereas the lower path describes the formation of loose or random aggregates which are defined by partial aggregation of the fluorinated endgroups. Both pathways lead to an infinite network at the final stage of the aggregation process.

ence of the coupling group isophorone diisocyanate mentioned in the Introduction which we cannot determine separately. This results in a volume fraction of $\Phi_{Gel} = 0.066$ and 0.063 for PEG−$(C_6F_{13})_2$ and PEG−$(C_8F_{17})_2$, respectively. If the polymer density is known, we can now easily calculate the polymer concentration. Strictly speaking, the polymer density of both systems is not known. Neglecting the endgroups in that estimate, we use the density of highly crystalline PEG [$\rho_{PEG} = 1.23$ g/cm^3].[31] With this information and the following formula

$$c_{gel} = \frac{\Phi_{gel}\rho_{PEG}}{1 - \Phi_{gel}} 100 \qquad (5)$$

the gel concentrations are $c_{gel} = 8.6$ wt % and $c_{gel} = 8.3$ wt % for PEG−$(C_6F_{13})_2$ and PEG−$(C_8F_{17})_2$, respectively, at room temperature. These calculated gel concentrations c_{gel} correspond remarkably well to the experimentally determined concentrations of 9.8 wt % and 9.6 wt % for PEG-$(C_6F_{13})_2$ and PEG-$(C_8F_{17})_2$, respectively, where only aggregated endgroups could be detected by ^{19}F transverse relaxation (Figure 2). Gelation is usually ascribed to the formation of macroscopic bridges in the system. Therefore, we conclude that infinite networks are formed in both polymer solutions around 10 wt %. Remarkably, this is also the concentration, for which we no longer can detect loose (or dangling) chain ends.

Thus, complete aggregation seems to be related to the formation of an infinite network rather than local features such as flower micelles. Of course, we cannot tell if the network is built up by loops and bridged chains or only by bridged chains.

Temperature Dependence of Aggregation. The second set of experiments involves the temperature dependence of the fraction of nonaggregated and weakly aggregated chain ends. This is determined by the chemical shift of one fluorinated endgroup. The chemical shift is sensitive toward the chemical environment (water or fluorocarbon aggregates or both) of the endgroup. In our experiments, the concentration of nonaggregated and weakly aggregated species increases over the temperature range studied. The aggregated chain

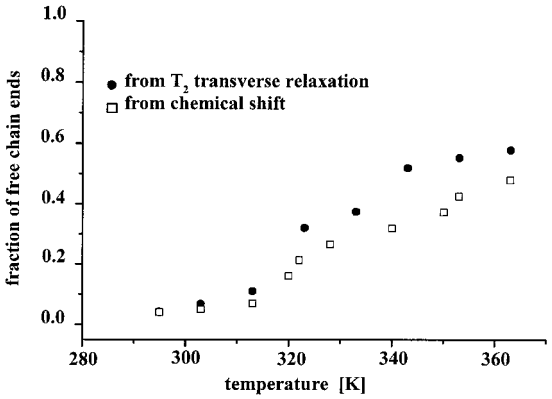

Figure 7. Fractions of free chain ends of PEG−$(C_6F_{13})_2$ with $c_{pol} = 9.6$ wt % as a function of temperature determined from ^{19}F NMR transverse relaxation and ^{19}F NMR chemical shift. With increasing temperature, both sets of data show an cascade increase of the fraction of free chain ends.

ends leave the core or are partially aggregated, as was described above for "loose" aggregates. The chemical environment of aggregated species change continuously with the temperature. In the case of the high-concentration sample, the complete network is broken into smaller aggregated species and free chain ends.

By changing the temperature, we find a marked effect on the aggregation process. This can only happen if the solutions are close to the thermodynamic borderline of aggregated versus free chain ends. Therefore, by increasing kT about 25% from 295 to 370 K, the small change in energetic units as shown above corresponds to a strong impact on the aggregation process.

Comparison of the Results of Different ^{19}F NMR and Rheological Experiments. Because both types of ^{19}F NMR experiments are able to determine the aggregation of the fluorinated endgroups, we finally compare the methods in Figure 7 for a high concentration sample PEG−$(C_6F_{13})_2$ with a high signal-to-noise-ratio. At room temperature ($T = 295$ K) both methods coincide because we used the aggregation of 95% as determined from transverse relaxation as a reference for the chemical shift. Both methods show the same trend, but with increasing temperature, the curves systematically deviate from each other where the transverse relaxation experiment gives higher values for the free chain ends. This can be attributed to the fact that the chain ends in the aggregate core are subject to residual dipolar couplings.[20] Thus, the corresponding signals are not completely refocused by the 180° pulse, and to get the actual amount of free chain ends, we need to correct the relaxation data by a factor of 15%. This number was estimated by comparing the intensities of the FID and the echo produced after a 90°−180° pulse sequence at all temperatures. Moreover, the line widths observed in the spectra (1−5 ppm) are considerably broader than those expected from a Lorentzian line width with $T_2 = 2$ms. Thus, the exchange between aggregated and free chain ends leading to an averaged chemical shift may not be complete, and the fraction of the free ends would then be higher than those deduced from the chemical shift. Nevertheless, we would like to stress that whenever possible the aggregation behavior should be examined through different NMR parameters in order to obtain reliable results.

Last, but not least, the exchange time τ_e between aggregated and loose ends can be determined rather accurately by combining the results from transverse

relaxation and from chemical shift measurements: From the former, τ_e must fulfill the condition $\tau_e \geq 200\ \mu s$. From the fact that averaged chemical shifts and broad lines are observed, τ_e must fulfill the condition $\tau_e \leq 500\ \mu s$; see Slichter,[18] Appendix F. Therefore, $200\ \mu s \leq \tau_e \leq 500\ \mu s$. Thus τ_e is shorter than the characteristic time scales of the rheological measurements previously reported[1] for the same systems, which are above 1 ms. This means that the viscosity only probes average behavior of chain ends between free and aggregated states.

We also mention that a major difference between the two polymers is their zero shear viscosity at 20 °C (see Xu et al.,[1] Figure 4). At 6 wt %, the C8 polymer has a viscosity on the order of 200 Pa·s, whereas the C6 polymer has a viscosity closer to 20 Pa·s. This paper argues that at this concentration the moduli are similar and the lower viscosity of the C6 polymer comes from a more than 10-fold faster exchange time (2 vs 80 ms at 5 to 6 wt %). Our present work shows, however, that at such concentrations the degree of aggregation of the two polymers as determined on a shorter time scale is markedly different; see Figure 2. Moreover, although our data indicate a major difference in the concentration dependence of aggregation for the two polymers, the viscosity data are similar, apart from a constant factor. Thus, the relation between the two phenomena remains to be clarified.

Concluding Remarks

^{19}F NMR experiments are able to probe the aggregation behavior of telechelic partially fluorinated polymer systems in water. The aggregation of the fluorinated endgroups increases with increasing polymer concentration, which can be monitored by the short transverse relaxation time $T_{2,short}$ and the fraction A_{short} belonging to it. The infinite network is reached at ca. 10 wt % for both polymer systems studied and is defined by the complete aggregation of all endgroups. The experimental results are consistent with the simulation results for symmetric triblock copolymers A−B−A.

With temperature-dependent ^{19}F NMR chemical shift measurements, the self-organization of a fluorocarbon polymer in solution can likewise be studied. The observed chemical shift is interpreted as resulting from a mixture of aggregated and nonaggregated/weakly aggregated fluorocarbon endgroups. In our nonionic polymer system, we found a marked increase of the free and weakly aggregated fluorocarbon endgroups with increasing temperature.

Finally, polymer surfactants differ from "normal" surfactants in the last stage of the aggregation process by building up an infinite network.

Acknowledgment. We thank Manfred Hehn and Hans-Peter Raich for building the ^{19}F NMR probehead and Prof. Peter Macdonald for carefully checking the manuscript. M.A.W. acknowledges financial support from the Alexander von Humboldt Foundation through a Senior Research Award.

References and Notes

(1) Xu, B.; Lie, L.; Yenta, A.; Misaim, Z.; Kanagalingam, S.; Winnik, M. A.; Zhang, K.; Macdonald, P.; Menchen, S. *Langmuir* **1997**, *13*, 2447.
(2) Lüsse, S.; Arnold, K. *Macromolecules* **1996**, *29*, 4251.
(3) Alami, E.; Almgren, M.; Brown, W. *Macromolecules* **1996**, *29*, 5026.
(4) Walderhaug, H.; Hansen, F. K.; Abramsen, S.; Persson, K.; Stilbs, P. *J. Phys. Chem.* **1993**, *97*, 8336.
(5) Yekta, A.; Xu, B.; Duhamel, J.; Adiwidjaja, H.; Winnik, M. A. *Macromolecules* **1995**, *28*, 956.
(6) Nyström, B.; Walderhaug, H.; Hansen, F. K. *J. Phys. Chem.* **1993**, *97*, 7743.
(7) Abrahmsen-Alami, S.; Stilbs, P. *J. Phys. Chem.* **1994**, *98*, 6359.
(8) Bieze, T. W. N.; van der Maarel, J. R. C.; Eisenbach, C. D.; Leyte, J. C. *Macromolecules* **1994**, *27*, 1355.
(9) Borisov, O. V.; Halperin, A. *Macromolecules* **1996**, *29*, 2612.
(10) Semenov, A. N.; Joanny, J. F.; Khokhlov, A. R. *Macromolecules* **1995**, *28*, 1066.
(11) Hiemenz, P. C. *Principles of Colloid and Surface Chemistry*; Marcel Dekker, Inc.: New York, 1986.
(12) Israelachvili, J. *Intermolecular & Surface Forces*; Academic Press: London, 1992.
(13) Brandrup, J.; Immergut, E. H. *Polymer Handbook*; J. Wiley & Sons: New York, 1992.
(14) Devanand, K.; Selser, J. C. *Macromolecules* **1991**, *24*, 5943.
(15) Schmidt-Rohr, K.; Spiess, H. W. *Multidimensional Solid-State NMR and Polymers*; Academic Press: London, 1994.
(16) Callaghan, P. T. *Principles of Nuclear Magnetic Resonance Microscopy*; Clarendon Press: New York, 1991.
(17) Fukushima, E.; Roeder, S. B. W. *Experimental Pulse NMR*, Addison-Wesley Publishing Company: Reading, MA, 1981.
(18) Slichter, C. P. *Principles of Magnetic Resonance*; Springer-Verlag: Berlin, 1978.
(19) Bloembergen, N.; Purcell, E. M.; Pound, R. V. *Phys. Rev.* **1948**, *73*, 679.
(20) Cohen-Addad, J. P. *NMR and Fractal Properties of Polymeric Liquids and Gels*, Vol. 25, Part 1; Pergamon Press: Oxford, 1993.
(21) Cochin, D.; Hendlinger, P.; Laschewsky, A. *Colloid Polym. Sci.* **1995**, *273*, 1138.
(22) Fung, B. M.; Mamrosh, D. L.; Rear, E. A.; Frech, C. B.; Afzal, J. *J. Phys. Chem.* **1988**, *92*, 4405.
(23) Guo, W.; Brown, T. A.; Fung, B. M. *J. Phys. Chem.* **1991**, *95*, 1829.
(24) Guo, W.; Li, Z.; Fung, B. M.; Rear, E. A.; Harwell, J. H. *J. Phys. Chem.* **1992**, *96*, 6738.
(25) Guo, W.; Fung, B. M.; Rear, E. A. *J. Phys. Chem.* **1992**, *96*, 10068.
(26) Raspaud, E.; Lairez, D.; Adam, M.; Carton, J.-P. *Macromolecules* **1994**, *24*, 2956.
(27) Ngyuen-Misra, M.; Mattice, W. L. *Macromolecules* **1995**, *28*, 1444.
(28) Ngyuen-Misra, M.; Misra, S.; Wang, Y.; Rodriguez, K.; Mattice, W. L. *Prog. Colloid Polym. Sci.* **1997**, *103*, 138.
(29) Pfüller, U. *Mizellen, Vesikel, Mikroemulsionen*; Springer-Verlag: Berlin, 1986.
(30) Shinoda, K.; Hato, M.; Hayashi, T. *J. Phys. Chem.* **1972**, *76*, 909.
(31) Molyneux, P. *Water-Soluble Synthetic Polymers*, Vol. 1; CRC Press: Boca Raton, FL, 1984.

MA9818735